

Pinch Effect in a Germanium Electron-Hole Plasma

V. N. Dobrovolskii and M. N. Vinoslavskii

Kiev State University

Submitted November 10, 1971

Zh. Eksp. Teor. Fiz. 62, 1811-1817 (May, 1972)

The conductivity of an injected germanium electron-hole plasma is investigated when the power supplied to the plasma exceeds considerably the critical Bennett value (up to 400 kW/cm). A magnetothermal and a thermal pinch effects are observed. The channel radius of the magnetothermal pinch, its conductivity, electron and hole concentration at the instant preceding melting of the channel, are determined. The duration of various stages of the pinch effect are estimated. The data obtained are in good agreement with the theoretical concepts regarding the pinch effect.

1. INTRODUCTION

THE pinch effect in semiconductors has been observed only in indium antimonide at low temperatures^[1-4]. The high electron mobility makes it possible to satisfy in this case the Bennett condition^[5,6] in simplest fashion without a noticeable heating of the sample. The carrier lifetime in indium antimonide is short (usually on the order of or shorter than the duration of the current pulse), so that the pinch effect is accompanied by an appreciable recombination of the electrons and holes. The recombination smooths out the effect of plasma redistribution, makes the theory more complicated, and makes the comparison of the experimental results with the theory more difficult.

A clear-cut manifestation of the pinch effect and a smaller influence of recombination in this effect can be expected in semiconductors with long lifetimes, if it is possible to maintain in these semiconductors, without damaging the sample, the critical value^[5] of the power fed to the plasma during the course of time necessary to form the pinch channel, or a larger value of the power. In this respect, greatest interest attaches to germanium^[7], where a long lifetime and appreciable mobility of the carriers is possible.

We describe here the occurrence of magnetothermal and thermal pinches (see^[6] for the classification) in an injected germanium plasma at room temperature.

2. EXPERIMENTAL RESULTS

We used cylindrical n-germanium samples with resistivity 40 ohm-cm and carrier displacement diffusion length 0.15 cm. The dimensions (length l and diameter d) of typical samples are shown in the table. An indium p-n junction was fused into one of the ends of the sample, and an antibarrier tin contact was produced on this junction. To decrease the rate of surface recombination, the sample was etched in boiling perhydrol. A long-persistence oscilloscope was used to obtain oscillograms of the current I flowing through the sample after application of a single voltage pulse U of duration $\tau_{\text{pulse}} = 18$ or 50 msec in the transmission direction. The pulse waveform was close to rectangular, namely, the variation of U during the time of the pulse did not exceed 20% relative to the voltage at the start of the pulse. Typical current oscillograms at different values of U are shown in Fig. 1. At small values of the power $N = IU$ fed to the sample (small U), a monotonic increase of the current during the entire pulse, due to the plasma injection, was ob-

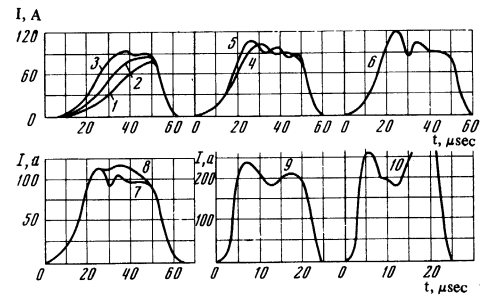


FIG. 1. Oscillograms of current I at different pulse voltages. Sample No. 5: 1) $U = 115$ V, 2) 130 V, 3) 150 V, 4) 160 V, 5) 175 V, 6) 185 V, 7) 180 V, 8) sample placed in a longitudinal magnetic field 650 Oe, $U = 180$ V. Sample No. 1: 9) $U = 300$ V, 10) 400 V. The values of U are given for the instant of maximum current through the sample, t is the time.

served (oscillograms 1 and 2). After N reached during the time of the pulse a certain value N_c , the growth of the current gave way to a decrease. Oscillations were usually observed in this case (oscillograms 3-6). A weak longitudinal magnetic field eliminated the effect of decreasing current (oscillograms 7 and 8).

Further increase of the voltage supplied to the sample led to a growth of the current at the end of the pulse. This growth was observed particularly strongly in the case of voltage pulses with $\tau_{\text{pulse}} = 18 \mu\text{sec}$ (oscillogram 9). When the voltage was gradually increased, we were able to obtain a value at which the growth of the current at the end of the pulse could be observed in reproducible fashion many times. However, an increase of the voltage by (10-20)% above this value led to a sharper increase of the current, non-reproducibility of the oscillograms, and sometimes to the appearance of longitudinal cracks on the sample. At sufficiently high voltages (oscillogram 10), the cracking was accompanied by ejection of the molten metal of the sample (Fig. 2). In this case cutting the sample revealed an empty channel due to melting (Fig. 3). The channels were of round cross section; the radii r_t of the channels melted in samples 2 and 3 are indicated in the table.

In some cases when the current increased, the sample was spontaneously cleaved at the end of the pulse in longitudinal direction. A recrystallized channel was observed in the central part of the cleavage. There was no channel at the contacts, at distances up to ~ 0.1 cm. The table lists the radii of the channels produced in samples 4 and 6. Several samples in which growth of the current at the end of the pulse was observed were

No.	l , cm	d , cm	τ_p , μsec	I_c , A	W_c , kW/cm	I_m , A	W_t , kW/cm	$2l_t$, cm	$\sigma_t \cdot 10^{-3}$, $\Omega^{-1} \text{cm}^{-1}$	I_f^{theor} , A
1	0.36	0.32	18	200	250	170	260			
2	0.30	0.24	»	185	220	260	390	0.013	1.3	390
3	0.40	0.24	»	»	»	140	225	0.010	1.1	300
4	0.40	0.24	»	»	»	125	135	0.0093	1.7	279
5	0.40	0.24	50	97	50					
6	0.20	0.11 × 0.11 *	»	53	45	40	43	0.0031		93

*Sample No. 6 had a quadratic cross section.



FIG. 2

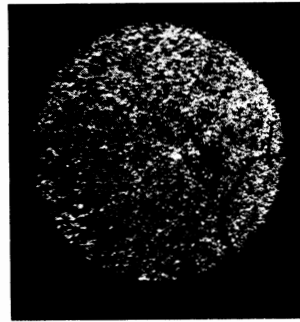


FIG. 3

FIG. 2. Ejection of molten material from sample No. 1
 FIG. 3. Hollow melted channel in sample No. 2. The channel passes through at an angle to the plane of the sample cross section.



FIG. 4



FIG. 5

FIG. 4. Recrystallized channel in a spontaneously cleaved sample.
 FIG. 5. "Craters" in a specially cleaved sample.

specially cleaved transversely to the axis by prolonged passage of a small current. "Craters" were observed on the cleavage (Fig. 5). No such "craters" were observed on cleaved samples through which no strong electric pulses were passed. The "crater" production is apparently connected with melting of the sample during the action of the pulse. When the lengths of samples with 0.24 cm diameter was decreased to $l \sim 0.15$ cm, the effects described above were not observed. In samples of the same length but of smaller cross section ($\sim 0.1 \times 0.1$ cm), these effects were observed. The table lists, for different samples, the values of the current I_c at which the current in the sample begins to decrease (oscillogram 3 of Fig. 1) and the values of the current I_t at the minimum (oscillogram 10).

Using a movable probe, we plotted at fixed instants of time the distribution of the potential V along the sample. Curve 1 of Fig. 6 was obtained for $N < N_c$ in the case when there was no decrease of the current. Curves 2 and 3 were obtained for $N \gtrsim N_c$ in the pres-

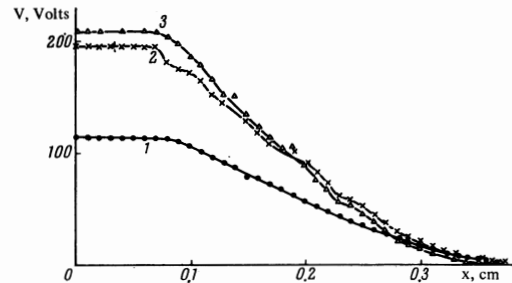


FIG. 6. Distribution of potential V along the sample: \bullet — $N = 4.6$ kW $< N_c$ in the absence of a decrease in the current at the instant when its maximum value is established; \square and Δ — $N \gtrsim N_c = 17$ kW in the presence of a decrease of the current at the instants of its maximum and subsequent minimum values, respectively.

ence of a decrease. Such plots have made it possible to determine the intensity of the electric field E and the power $W = IE$ at different points of the sample. E and W are maximal in the central part of the sample. The power W delivered to the central part of various samples at the instants of time indicated above, at the start of the decrease of the current (W_c), and at its minimum (W_t) are all listed in the table.

3. DISCUSSION OF RESULTS

The decrease of the current at $N \geq N_c$ can be attributed to a pinch effect produced in the sample and an ensuing decrease of the sample conductivity^[1]. This pinch-induced decrease of the current is accompanied by current oscillations, just as in a similar situation in indium antimonide (cf., e.f.,^[6,8]). The oscillations in the plasma lead to oscillations of the voltage distribution along the sample. There are no oscillations due to the pinch and no decrease of the current in a longitudinal magnetic field (Fig. 1, oscillograms 7 and 8), because the pinch is destroyed by the helical instabilities^[9]. The growth of the current at the end of the pulse, and the formation of a molten channel, can be naturally attributed to the heating of the channel and to the development of a magnetothermal pinch followed by a thermal pinch. The field near the contacts is weak (Fig. 6), so that no channel is produced there. The absence of a pinch effect in short samples is due to the fact that the plasma injection, which occurs over the entire area of the contact, prevents the pinching of the plasma in the region adjacent to the contact^[8,10].

Let us compare quantitatively our data with the theoretical notions concerning the pinch effect.

a) Formation of the pinch channel. The critical power necessary for the pinch effect to arise^[5] is equal to

$$W_{cr} = (IE)_{cr} = \frac{2k(T_n + T_p)c^2}{e(\mu_n + \mu_p)}$$

μ_n and μ_p are the electron and hole mobilities, T_n and T_p are the temperatures of the electron and hole gases, K is Boltzmann's constant, c is the speed of light, and e is the electron charge. For $T_n = T_p = T = 293^\circ$ (T is the lattice temperature) we have $W_{CR} = 17$ kW/cm. When the Joule and field-induced^[11] heating of the electron and hole gases by the instant when the decrease of the current begins are taken into account, we obtain $W_{CR} = 22-25$ kW/cm. The Joule heating increased the temperature by 3-6% and the field heating by 10-30%. The carrier density in the central part of the sample, at the initial instant of current decrease, was $10^{15}-10^{16}$ cm⁻³. According to^[12], electron-hole scattering changes the mobility little under these conditions, and is disregarded in the calculation of W_{CR} .

The power W_C , at which the current decrease due to the pinching of the plasma is observed, is larger than W_{CR} for all samples (see the table). The pinching begins when the power $W = IE$ becomes equal to W_{CR} , and affects the value of the current only after an appreciable compression of the plasma has taken place. The compression time is on the order of $\tau_C = c^2 d^2 / 16 \mu_n \mu_p W^{[13]}$. If $\tau_C > \tau_{pulse}$ then, in spite of satisfaction of the Bennett condition, the plasma does not manage to become pinched during the time τ_{pulse} of the voltage pulse and no decrease of the current is observed. At $W = W_{CR}$ we had $\tau_C = \tau_C^{CR} \approx 50$ μ sec in sample No. 1, ≈ 25 μ sec in samples 2-5, and 6 μ sec in sample No. 6. The condition $\tau_C^{CR} > \tau_{pulse}$ was satisfied for samples 1 and 2, and the inverse conditions for samples 5 and 6. This explains qualitatively why W_C exceeds W_{CR} by approximately one order of magnitude in the former case, and W_C is much closer to W_{CR} in the latter case.

b) Heating of the pinch channel. The power dissipated in a unit length of the plasma filament is

$$W_q = 2\pi r_f \kappa dT / dr, \quad (2)$$

where κ is the thermal conductivity coefficient and r_f is the radius of the pinch filament. At small r_f we have $dT/dr \approx T/r_f$. Assuming $\kappa = 150/T$ [W/cm]^[14], we obtain $W_q = 0.9$ kW/cm. $W_q \ll W_{CR}$ and all the more W_C . At small r_f , the power delivered to the sample is consumed mainly in heating the plasma pinch only. This causes a rapid heating of the channel, followed by melting. Since the heating and melting increase the conductivity of germanium^[15,16], it is natural to assume that the start of the intense heating corresponds to the minimum on the current oscillogram (Fig. 1, oscillograms 9 and 10). At this instant, the current I_t flows through the sample and a power W_t is delivered to the central part of the sample. The melting of the channel is not necessarily accompanied by destruction of the sample. This is evidenced by the reproducibility of oscillograms such as oscillogram 9 of Fig. 1, and the observation of craters in specially cleaved samples (Fig. 5). One should expect inevitable damage to the sample if the temperature in the channel reaches the boiling temperature of germanium.

The heating of the channel proceeds through the following stages: heating without melting—magnetothermal pinch (with lifetime τ_{mt}), melting of the channel—thermal pinch (τ_t), further heating to the

boiling temperature (τ_b), and sample damage. The heat balance, assuming $r_f \approx r_t$, enables us to estimate the durations of the different stages. For the typical case of sample 3 we have $\tau_{mt} \approx 0.5$ μ sec, $\tau_t \approx 1$ μ sec, and $\tau_b \approx 1$ msec. The sum $\tau_{mt} + \tau_t + \tau_b \approx 2.5$ μ sec is of the same order as the time interval 5 μ sec elapsed in this case from the start of the current growth to the sample damage accompanied by ejection of molten material.

c) Characteristics of the magnetothermal-pinch channel. We do not know the temperature and density of the carriers in the channel, nor its radius, at any arbitrary instant of time. For the instant preceding the melting we can assume that $T_f = T_m = 1210^\circ$ K (the melting point of germanium) and $r_f = r_t$ is equal to the radius of the molten channel. Owing to the large lattice temperature we have $T_n = T_p = T_f$. The time τ_{mt} is much longer than the carrier lifetime in germanium at high temperature. According to the formulas of^[17], at $T = T_m$, the impact recombination, which is the most effective at high carrier densities, leads to a lifetime on the order of 0.001 μ sec. Therefore, at any rate during the final stage of the development of the magnetothermal pinch, the average carrier density n_f realized in the channel is close to the thermodynamic-equilibrium value n_0 . At the melting temperature we have $n_0 = 1.72 \times 10^{19}$ cm⁻³^[16].

The sharp increase of the current (osc. 9 and 10 of Fig. 1) may be due either to the development of a magnetothermal pinch or with the start of melting. In the former case the section of the oscillogram corresponding to the magnetothermal pinch is located immediately past the minimum of the current, and in the latter case ahead of the minimum. It is impossible to choose between these two cases, since we do not know the character of the variation of the current through the channel during the time of the magnetothermal pinch. It is determined by the simultaneous action of a number of factors that act in different directions (the changes of μ_n , μ_p , n_f , and r_f), the relative influences of which on the current are difficult to evaluate. Regardless of the particular case realized, however, the weak variation of the current in the region of the minimum during the time τ_{mt} enables us to assume, with a small relative error, that the current through the channel of the magnetothermal pinch is $I_f = I_t$.

The experimental data make it possible to determine the specific conductivity in the channel $\sigma_t = I_t / \pi r_t^2 E_t$ at the instant preceding the melting. The obtained values are given in the table. Their good agreement with the thermodynamic-equilibrium conductivity of germanium at the melting temperature, 1.25×10^3 ohm⁻¹cm⁻¹^[15], confirms the correctness of the conclusions drawn concerning the numerical characteristics of the magnetothermal-pinch channel.

d) Comparison of experimental magnetothermal-pinch characteristics with theory. The radius of the magnetothermal-pinch channel decreases in time. We can assume for this process a characteristic time $\tau_f = c^2 r_f^2 / 4 \mu_n \mu_p W$. During this time the plasma pinch with radius r_f is compressed to zero by the magnetic forces alone. An estimate shows that when the temperature in the channel rises from room temperature to the melting point, τ_f varies in the range 0.003-0.7 μ sec

$\lesssim \tau_{\text{mt}}$ (sample No. 3). The magnetothermal pinch is quasistationary.

Under the usual assumptions^[18,19] we have for a nondegenerate electron-hole plasma

$$\frac{I_f^2}{2\pi c^2 r_f^2} = 2n_f kT_f. \quad (3)$$

The quantity on the left is the pressure of the magnetic field on the pinch-channel boundary, and on the right is the gas-kinetic pressure.

Formula (3) was used to determine the currents I_f^{theor} corresponding to the values of T_f , n_f , and r_f defined in Sec. c for the instant preceding the melting. Their values for different samples are given in the table. The currents I_f^{theor} are in reasonable agreement with the experimental currents I_t .

The width of the forbidden band decreases with increasing temperature^[17]. The temperature gradient results therefore in certain nonmagnetic forces striving to displace the plasma from sample sections with lower temperature into sections where the temperature is higher. The pinch-channel temperature is higher than that of the rest of the sample. Consequently, these forces act on the plasma in the same direction as the magnetic forces producing the pinch. This circumstance was not taken into account in the derivation of (3). It may be the reason why I_f^{theor} is higher I_t . At $T = T_M$ the Fermi level is located 1.52 kT away from the bottom of the conduction band and 0.93 away from the top of the valence band. Using this position of the Fermi level, I_f^{theor} was determined from a formula similar to (3) but valid for any degree of degeneracy. The obtained values differ from those listed in the table by only several per cent.

The authors thank V. V. Vladimirov for a discussion of the work.

- ¹M. Glicksman and M. C. Steele, Phys. Rev. Lett. **2**, 461 (1959).
- ²B. D. Osipov and A. N. Khvoshchev, Zh. Eksp. Teor. Fiz. **43**, 1179 (1962) [Sov. Phys.-JETP **16**, 833 (1963)].
- ³B. Ancker-Johnson and J. E. Drummond, Phys. Rev. **131**, 1961 (1963).
- ⁴A. P. Shotov, S. P. Grishechkina, and R. A. Muminov, Zh. Eksp. Teor. Fiz. **50**, 1525 (1966) [Sov. Phys.-JETP **23**, 1017 (1966)].
- ⁵W. H. Bennett, Phys. Rev. **45**, 897 (1934).
- ⁶B. Ancker-Johnson, IX Mezhdunarodnaya konferentsiya po fizike poluprovodnikov (IX International Conference on the Physics of Semiconductors), Vol. II, Nauka, 1969, p. 859.
- ⁷A. E. Stefanovich, Fiz. Tverd. Tela **9**, 2035 (1967) [Sov. Phys.-Solid State **9**, 1598 (1968)].
- ⁸A. P. Shotov, I. I. Zasavitskiĭ, B. N. Matsionashvili and R. A. Muminov, IX Mezhdunarodnaya konferentsiya po fizike poluprovodnikov (IX International Conference on the Physics of Semiconductors), Vol. II, Nauka, 1969, p. 891.
- ⁹B. B. Kadomtsev and A. V. Nedospasov, J. Nucl. Energy C **1**, 230 (1960).
- ¹⁰V. V. Vladimirov, Zh. Eksp. Teor. Fiz. **55**, 1288 (1968) [Sov. Phys.-JETP **28**, 675 (1969)].
- ¹¹E. M. Conwell, Transport Properties, Suppl. 9 of Solid State Physics, ed. by F. Seitz and D. Turnbull, Academic, 1967.
- ¹²M. B. Prince, Phys. Rev. **93**, 1204 (1954).
- ¹³M. Glicksman, Jap. J. Appl. Phys. **3**, 354 (1964).
- ¹⁴J. R. Drabble and H. J. Goldsmit, Thermal Conduction in Semiconductors, Pergamon, 1961.
- ¹⁵V. M. Glazov, S. N. Chizhevskaya, and N. N. Glagoleva, Zhidkie poluprovodniki (Liquid Semiconductors), Nauka, 1967.
- ¹⁶F. J. Morin and J. P. Maita, Phys. Rev. **94**, 1525 (1954).
- ¹⁷J. S. Blakemore, Semiconductor Statistics, Pergamon, 1961.
- ¹⁸L. A. Artsimovich, Upravlyamye termoyadernye reaktsii (Controlled Thermonuclear Reactions), Fizmatgiz, 1961. [Gordon and Breach, 1964].
- ¹⁹G. Akramov, Dokl. Akad. Nauk SSSR **161**, 554 (1965) [Sov. Phys.-Dokl. **10**, 234 (1965)].

Translated by J. G. Adashko
208